Thermochimica Acta, 45 (1981) 39—48
Elsevier Scientific Publishing Company, Amsterdam — Printed in Belgium

SOLID-STATE REACTIONS BETWEEN ALKALI PERSULFATES AND OXIDES OF CORUNDUM STRUCTURE

HAMID J. JAFFER and FADHIL JASIM *

Department of Chemistry, College of Science, Baghdad University, Baghdad (Iraq)

(Received 2 October 1980)

ABSTRACT

The effects of three corundum structure oxides, α-Al_2O_3, α-Cr_2O_3, and α-Fe_2O_3, on the thermal decomposition of sodium and potassium peroxodisulfates (persulfates) under non-isothermal static air conditions and using various oxide/persulfate molar ratios, have been thermoanalytically investigated. Compounds such as $Na_3Al(SO_4)_3$, $K_3Al(SO_4)_3$, $Cr_2(SO_4)_3$, $K_3Cr(SO_4)_3$, and $Na_3Fe(SO_4)_3$ are identified by X-ray diffractometry and conventional chemical analysis. The molar ratios as well as temperatures of the stoichiometric formation for these compounds have been established. At higher temperatures, α-Al_2O_3 acts as a promoter catalyst for the decomposition of pyrosulfate to sulfate, whereas α-Cr_2O_3 behaves as a retarder for the decomposition of persulfate. A eutectic mixture is formed between $K_3Al(SO_4)_3$ and K_2SO_4 at 675°C. Also, $K_3Fe(SO_4)_3$ is identified as two crystalline phases.

INTRODUCTION

The three oxides, α-Al_2O_3, α-Cr_2O_3 and α-Fe_2O_3, belong to the corundum structure [1] in that they have rhombohedral hexagonally close-packed ionic crystals [2,3]. It is worth mentioning that the defect in the lattice structure is so small that no adequate analytical technique is available for its measurement [4]. Moreover, the *p*-type semiconductivity of α-Cr_2O_3 increases with the rise in number of defective sites of its lattice structure. Nevertheless, the oxide behaves as an electric conductor when heated to high temperatures [4]. Further, the semiconductive behavior of α-Fe_2O_3 is due to a defective lattice structure caused by the deficiency of oxygen atoms on both sides of the Fe^{3+} ion. Because of the presence of some impurities, iron(III) oxide may behave as a *p*- or *n*-type semiconductor. The catalytic effects of some oxides, including those mentioned above, on the thermal decomposition of the chlorate and perchlorate of potassium, as well as other salts, were studied [5—14].

Jasim and co-workers [15—24] studied high temperature reactions of binary systems of transition metals and lanthanide oxides with persulfates of sodium and potassium and found interesting results.

In this work we have studied the thermal reactions of six oxide—persulfate

---

* To whom correspondence should be addressed.

binary systems to establish the proper conditions for optimal catalysis, compound formation, phase transition, and thermal stabilities of intermediate and final products.

EXPERIMENTAL

Reagents, preparation of samples, thermal and X-ray diffraction analyses equipment were as described previously [20].

RESULTS AND DISCUSSION

Aluminium(III) oxide—persulfate systems

Figures 1 and 2 show the derivatograms of α-Al_2O_3—$Na_2/K_2S_2O_8$ for the molar ratios 1 : 6, 1 : 3, 1 : 2, 2 : 3, 1 : 1, and 4 : 3. Neither the TG nor the DTA curves indicate any significant effect of α-Al_2O_3 on the T_i and T_f of decomposition of sodium or potassium persulfate into pyrosulfate.

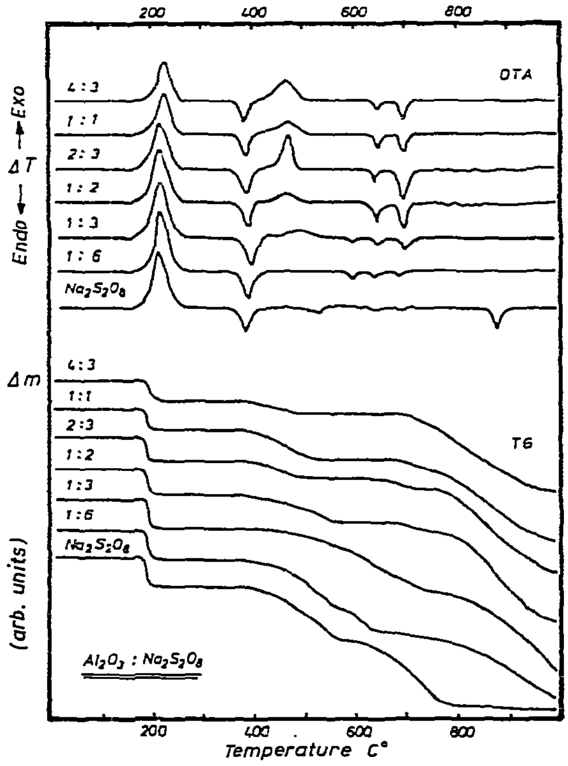

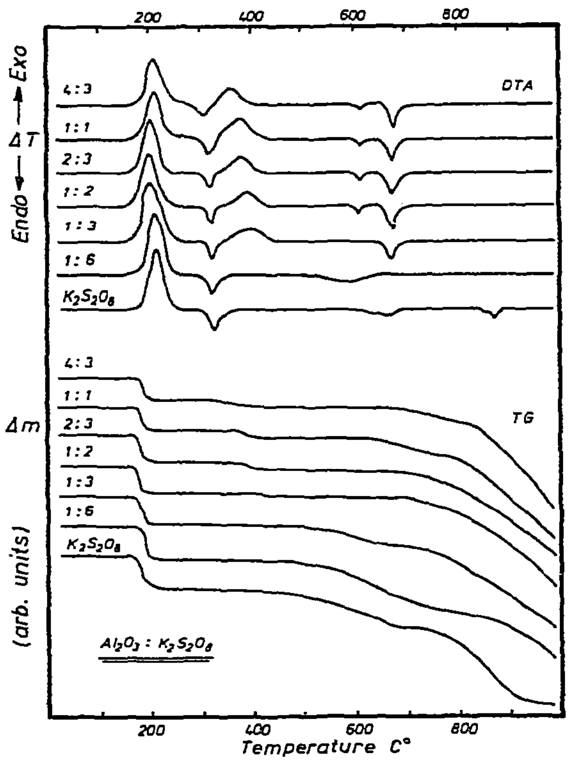

Fig. 1. TG and DTA curves of aluminium(III) oxide—sodium persulfate mixtures.

Fig. 2. TG and DTA curves of aluminium(III) oxide—potassium persulfate mixtures.

α-Al_2O_3—$Na_2S_2O_8$ system

The TG curves (Fig. 1) reveal that part of the thermally produced $Na_2S_2O_7$ undergoes thermal decomposition before reacting with α-Al_2O_3. Calculation proved that the loss in weight is proportional to the amount of persulfate already present in the mixture, except for the molar ratios 1 : 1 and 4 : 3, where the loss is not proportional (Table 1). Also, a horizontal plateau is seen on the TG curve of the stoichiometric ratio 2 : 3 between 510 and 670°C. Samples isolated at 520°C gave XRD patterns [*d*-lines (Å) = 3.12, 3.00, 3.93] which indicate the presence of relatively large amounts of $Na_3Al(SO_4)_3$ as well as traces of Na_2SO_4 and α-Al_2O_3. In the meantime, the DTA curves did not exhibit any change in the melting point of the pure $Na_2S_2O_7$ produced in the presence of the oxide, but after melting the T_i of $Na_2S_2O_7$ immediately lowers as the oxide content increases in the mixture. The stoichiometric equation for this reaction is

$$3\ Na_2S_2O_7 + Al_2O_3 \rightarrow 2\ Na_3Al(SO_4)_3$$

The presence of a little sodium sulfate, as traced by X-ray diffraction analysis, is due to the fact that some of the $Na_2S_2O_7$ decomposes before reacting with the oxide. However, the TG curve for the 2 : 3 ratio registers a weight loss of 4.5% between 670 and 700°C; the curve then levels off until 770°C. Samples sintered at 740°C when examined by X-ray diffractometry proved to be mainly $Na_3Al(SO_4)_3$, from which it can be safely deduced that this weight loss is attributed to a partial decomposition of this salt

$$2\ Na_3Al(SO_4)_3 \rightarrow 3\ Na_2SO_4 + Al_2O_3 + 3\ SO_3$$

This leads to the conclusion that the decomposition of the salt formed at the 2 : 3 ratio occurs in two consecutive stages, whereas in the 1 : 1 and 1 : 2 ratios the salt decomposes in one step only due to the presence of excess α-Al_2O_3 which accelerates its decomposition through catalysis.

The three endotherms observed on the DTA curve of the 1 : 6 ratio between 580° and 710°C is ascribable to thermal decomposition of $Na_2S_2O_7$ only. The first endo peak seen on the curves of the other ratios at 640°C concerns the melting point of impure pyrosulfate [16,25]; that at 695°C is the melting point of $Na_3Al(SO_4)_3$, which differs by 20°C from values found by Fedorov and Chang [25]. This difference is perhaps because we used the Paulik—Erdy method for estimating the melting point of the salt.

α-Al_2O_3—$K_2S_2O_8$ system

From calculations of the thermoanalytical curves (Fig. 2), it is shown that the reaction between the thermally produced pyrosulfate and α-Al_2O_3 is shifted to a lower temperature value as the oxide content increases, and reaches 320°C with the ratio 4 : 3. A small percent (1.5—4.5) of $K_2S_2O_7$ has been decomposed at this temperature. This is because the pyrosulfate starts decomposition after melting by an interval of 50°C [15], whence it has sufficient time to react with the oxide [18]. In the 1 : 2 stoichiometric ratio

TABLE 1

Accumulated data from thermoanalytical investigations of the six binary systems of the proper stoichiometric ratios, and XRD patterns of compounds obtained

Binary systems	Ratio	O_2 lost (mg)		Persulfate decomp. temp. (°C)		Reaction temp, T_i (°C)	Formula of compound formed	Thermal stability (°C)	XRD patterns d(Å)
		Calc.	Found	T_i	T_f				
α-Al_2O_3—$Na_2S_2O_8$	2 : 3	12.8	12.5	190	235	425	$Na_3Al(SO_4)_3$	510—770	3.12, 3.00, 3.93
α-Al_2O_3—$K_2S_2O_8$	1 : 2	11.83	11.5	185	225	335	$K_3Al(SO_4)_3$	335—675	3.25, 2.75, 7.45
α-Cr_2O_3—$Na_2S_2O_8$	1 : 3	11.08	11.00	158	230	398	$Cr_2(SO_4)_3$	350—670	5.92, 3.55, 2.751
α-Cr_2O_3—$K_2S_2O_8$	1 : 3	9.96	10.0	167	225	330	$K_3Cr(SO_4)_3$	330—760	3.24, 7.41, 2.76
α-Fe_2O_3—$Na_2S_2O_8$	1 : 3	10.98	10.50	198	235	385	$Na_3Fe(SO_4)_3$	385—665	3.19, 6.80, 3.04
α-Fe_2O_3—$K_2S_2O_8$	1 : 3	9.76	9.0	160	200	280	$K_3Fe(SO_4)_3$	280—700	3.30, 7.41, 2.78

the system α-Al_2O_3—$K_2S_2O_8$ reacts to form $K_3Al(SO_4)_3$

$$3\ K_2S_2O_7 + Al_2O_3 \rightarrow 2\ K_3Al(SO_4)_3$$

which is made obvious by the X-ray powder diffraction method (Table 1). As for samples sintered at 570°C, the XRD pattern also shows d(Å) lines for trace amounts of K_2SO_4 (2.90, 3.00, 2.87), and α-Al_2O_3 (2.07, 1.61, 3.47).

It becomes evident from calculation of the SO_3 gas liberated and X-ray analysis that potassium aluminium trisulfate decomposes slowly and continuously after melting up to the ceiling temperature of the heating program (1050°C)

$$2\ K_3Al(SO_4)_3 \rightarrow 3\ K_2SO_4 + Al_2O_3 + 3\ SO_3$$

The sharp endotherm obtained at 675°C is evidently attributed to the formation of a eutectic of this salt with the potassium sulfate produced [26].

Chromium(III) oxide—persulfate systems

Figures 3 and 4 show the DTA and TG curves, under static air atmosphere of various molar ratios of Cr_2O_3—$M_2S_2O_8$ systems, where M is either Na or K. Contrary to the above-mentioned systems, the decomposition of the persulfate occurs in two steps represented as two large exotherms in the DTA

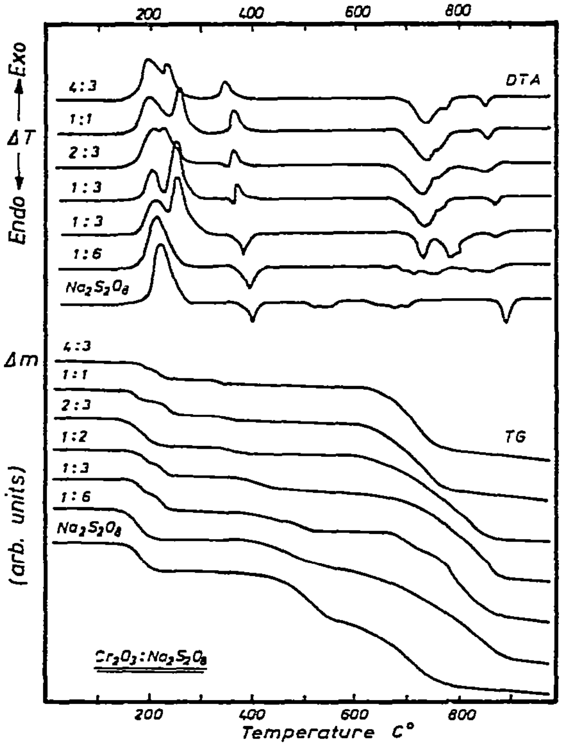

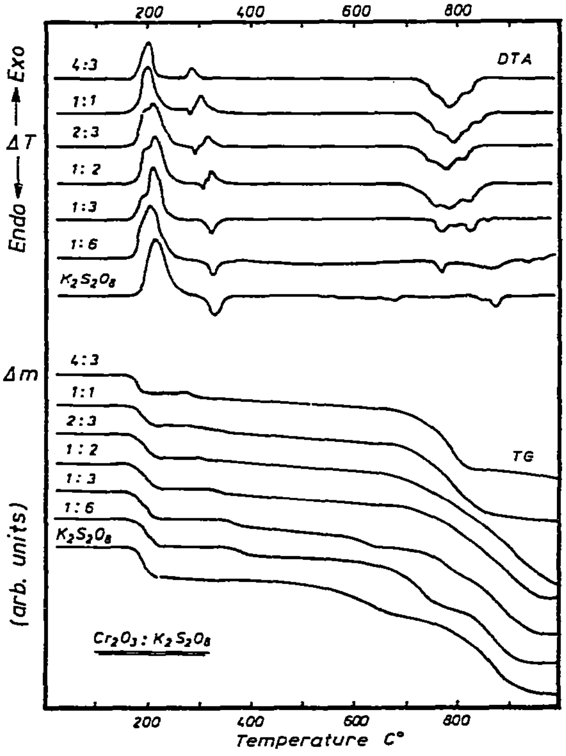

Fig. 3. TG and DTA curves of chromium(III) oxide—sodium persulfate mixtures.

Fig. 4. TG and DTA curves of chromium(III) oxide—potassium persulfate mixtures.

curves of Fig. 3, and as relatively small ones in DTA of Fig. 4. Also, the T_i values of the pure sodium or potassium persulfate decomposition were lowered and found to be 158 and 167°C, respectively. Since the two exotherms were not temperature resolved, it was rather difficult to sinter intermediates that give XRD patterns of known constitutions. However, the first exotherm could, perhaps, be ascribed to the partial decomposition of persulfate into pyrosulfate

$$M_2S_2O_8 \rightarrow M_2S_2O_7 + \tfrac{1}{2}\,O_2$$

as well as to a redox reaction

$$3\ M_2S_2O_8 + Cr_2O_3 \rightarrow 3\ M_2S_2O_7 + 2\ CrO_3$$

Thus the second exotherm may be imputed to thermal degradation of CrO_3 into Cr_2O_3 and oxygen atoms, and the latter combine through a secondary exothermic reaction [27—30]

$$4\ CrO_3 \rightarrow 2\ Cr_2O_3 + 3\ O_2$$

Further calculations indicate that the O_2 liberated is equivalent to that obtained from direct decomposition of equal amounts of pure persulfate.

Cr_2O_3—$Na_2S_2O_8$ *system*

Figure 3 shows that the melting point temperature of the thermally produced $Na_2S_2O_7$ is lowered to 348°C in the 2 : 3 ratio. The two peaks that appear on DTA curves at 338 and 350°C for the 1 : 1 and 4 : 3 ratios, respectively, suggest that the reaction proceeds before or during the melting of pyrosulfate. Here the T_i is lowered as the ratio increases and approaches a minimum at 338°C in the 4 : 3 ratio.

Further, the TG curves point out that part of the sodium pyrosulfate dissociates before reacting with the oxide. Thereafter, the reaction continues and the curves level off until $Cr_2(SO_4)_3$ formation stops. It is to be observed that the T_i—T_f of the reaction increases as the oxide content of the mixtures increases. On the other hand, X-ray analysis indicates that samples sintered at 620°C for the stoichiometric 1 : 3 molar ratio confirms the presence of $Cr_2(SO_4)_3$, Na_2SO_4, and a little Cr_2O_3. Computed data reveal that other ratios could not give relatively as high a percent yield of $Cr_2(SO_4)_3$, whence the stoichiometric reaction can be written as follows

$$3\ Na_2S_2O_7 + Cr_2O_3 \rightarrow Cr_2(SO_4)_3 + 3\ Na_2SO_4$$

Furthermore, XRD patterns (Table 1) for samples of various molar ratios heated at temperatures between 670 and 880°C suggest that the chromium(III) sulfate dissociates into Cr_2O_3 and SO_3 gas. It is to be observed from Fig. 3 that T_i—T_f values for this reaction are depressed by increasing the oxide proportion in samples. Moreover, the endo peak at the 1 : 6 ratio looks rather peculiar due to overlapping decomposition endotherms of $Cr_2(SO_4)_3$ and excess $Na_2S_2O_7$, whereas in the 1 : 3 ratio its decomposition proceeds in three neighboring steps, and in other ratios it occurs in two steps only [31]. It is worth noting that the presence of $Cr_2(SO_4)_3$ and Cr_2O_3 lowers the melting point of the 2 : 3 ratio to a minimum of 845°C.

Cr_2O_3—$K_2S_2O_8$ system

An exo peak is perceived on the DTA curves (Fig. 4) for the ratios 1 : 2, 2 : 3, 1 : 1, and 4 : 3, which is attributable to the exothermic reaction between $K_2S_2O_7$ and Cr_2O_3. Also, the T_i of the reacting system decreases when the oxide proportion increases. This exo peak disappears in the stoichiometric ratio of 1 : 3 due to the thermal neutrality [19]. Samples of this ratio heated at 700°C gave an XRD pattern (Table 1) which indicates the formation of $K_3Cr(SO_4)_3$ as well as traces of Cr_2O_3 and K_2SO_4

$$3\ K_2S_2O_7 + Cr_2O_3 \rightarrow 2\ K_3Cr(SO_4)_3$$

Also the T_i for the decomposition of this salt decreases as the ratio becomes greater, such as the 4 : 3 ratio where it is lowered to 685°C. Conversely, the T_f becomes higher and arrives at 995°C for the 2 : 3 ratio; at higher molar ratios, e.g. 4 : 3, it reaches 820°C. This behavior could be accounted for by the continuous formation of the potassium chromium trisulfate up to the 2 : 3 ratio with evolution of excessive amounts of heat, while in the 4 : 3 ratio the oxide increases and catalytically decomposes the salt; a reaction which absorbs heat depresses T_f.

Moreover, the multistage thermal decomposition of $K_3Cr(SO_4)_3$ is shown as a corrugated broad endotherm on the DTA curves. No explanation could be offered as to why its decomposition occurs in such small steps and not suddenly. This endotherm also shows that the greater the oxide present in the mixture, the shorter the interval of T_i—T_f.

However, samples heated at 1000°C for the various molar ratios give bright *d*-lines for Cr_2O_3 and K_2SO_4 mainly due to thermal degradation of the trisulfate

$$2\ K_3Cr(SO_4)_3 \rightarrow 3\ K_2SO_4 + Cr_2O_3 + 3\ SO_3$$

Iron(III)oxide—persulfate systems

The thermoanalytical curves of various molar ratios of oxide—persulfate systems are seen in Figs. 5 and 6. It is to be noted that the T_i for persulfate decomposition increases as the oxide—persulfate ratio becomes larger; a fact that is ascribed to the dilution effect of the oxide [19,32,33].

Fe_2O_3—$Na_2S_2O_8$ system

Figure 5 shows two exo peaks at 370 and 360°C for the ratios 2 : 3 and 4 : 3, respectively, indicating that their reactions occur before or during the melting of $Na_2S_2O_7$, where a part of the evolved heat of a reaction is absorbed by the endothermic decomposition of the pyrosulfate. It is also found that the T_i of the reactions of the two ratios is lowered by raising their oxide content. This may happen by catalytic action of excess oxide; however, calculation using the TG curves proves that the amount of $Na_2S_2O_7$ decomposed, before reacting with the oxide, is proportional to the persulfate content of the sample.

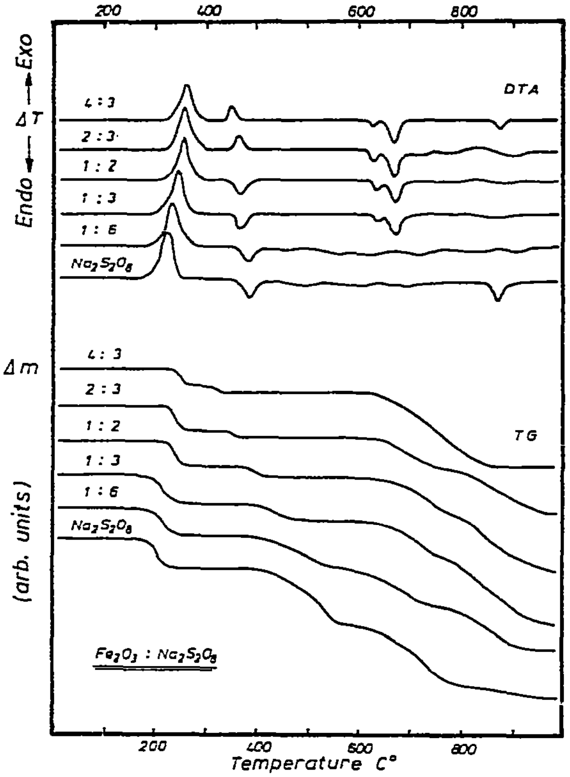

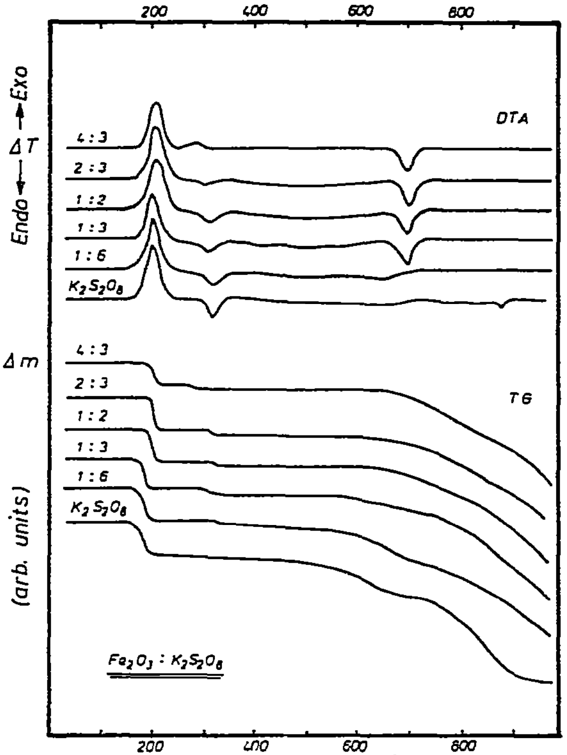

Fig. 5. TG and DTA curves of iron(III) oxide—sodium persulfate mixtures.

Fig. 6. TG and DTA curves of iron(III) oxide—potassium persulfate mixtures.

X-Ray powder analysis (Table 1) for samples heated at 620° C for the stoichiometric 1 : 3 ratio confirmed that $Na_3Fe(SO_4)_3$ constitutes a major part of the intermediate products. The trace amounts of Fe_2O_3 and Na_2SO_4 are due, respectively, to excess oxide present and the decomposition of unreacted pyrosulfate. Evidently there is the stoichiometric reaction

$$3\ Na_2S_2O_7 + Fe_2O_3 \rightarrow 2\ Na_3Fe(SO_4)_3$$

The same compound was recognized when samples of 2 : 3 and 4 : 3 ratios were heated at 520 and 530° C, respectively. Here the *d*-lines for Na_2SO_4 and Fe_2O_3 are brighter than those obtained in the case of the 1 : 3 ratio, which suggests a relatively lower yield of $Na_3Fe(SO_4)_3$.

The sodium iron trisulfate starts decomposition at 665° C

$$2\ Na_3Fe(SO_4)_3 \rightarrow 3\ Na_2SO_4 + Fe_2O_3 + 3\ SO_3$$

For greater molar ratios such as 4 : 3, the T_i—T_f for decomposition is rather squeezed where T_f approaches 865° C.

Careful observation of the DTA curves of the 1 : 3, 1 : 2, 2 : 3, and 4 : 3 ratios indicates two adjacent endotherms. That at 617° C belongs to the phase change of $Na_3Fe(SO_4)_3$, and the one at 665° C is a phase change due to melting and subsequent decomposition of the compound. Moreover, the area of the former endotherm reaches a maximum at the 2 : 3 ratio where the relative quantity of the salt is optimum.

For the 4 : 3 ratio the melting endotherm of Na_2SO_4 becomes clearest at 880° C. This is because the thermal decomposition of $Na_3Fe(SO_4)_3$, 665—865° C, takes place before the melting of the former.

Fe_2O_3—$K_2S_2O_8$ system

The melting point of $K_2S_2O_7$ is lowered as the ratios increase and is found to be 320, 316, 310, and 300° C for the ratios 1 : 6, 1 : 3, 1 : 2 and 2 : 3, respectively.

The exotherm at 280° C indicates that the reaction between the oxide and $K_2S_2O_7$ happens before or during the melting of the latter. Samples heated at 515, 600, and 680° C for the 1 : 3 ratio gave sharp *d*-lines (Table 1), identifying the presence of $K_3Fe(SO_4)_3$ [34]

$$3\ K_2S_2O_7 + Fe_2O_3 \rightarrow 2\ K_3Fe(SO_4)_3$$

in addition to a little K_2SO_4.

Other sharp *d*-lines (3.26, 2.76, 2.81 Å) of unknown identity (they have no counterpart in the ASTM cards) are shown which perhaps represent a new unknown phase of $K_3Fe(SO_4)_3$, which has a melting endotherm (Fig. 6) at 700° C.

Subsequently, the potassium iron(III) trisulfate dissociates in the conventional way

$$2\ K_3Fe(SO_4)_3 \rightarrow 3\ K_2SO_4 + Fe_2O_3 + 3\ SO_3$$

and its dissociation continues beyond the closing temperature of the heating program (1050° C).

REFERENCES

1 F.A. Cotton and G. Wilkinson, Advanced Inorganic Chemistry, Wiley—Interscience, New York, 1972, 3rd edn., p. 832.
2 F.A. Cotton and G. Wilkinson, Advanced Inorganic Chemistry, Wiley-Interscience, New York, 1972, 3rd edn., p. 262.
3 D. Nicholls, in A.F. Trotman-Dickinson (Exc.Ed.), Comprehensive Inorganic Chemistry, Vol. 3, Pergamon, Oxford, 1973, p. 666.
4 Per Kofstad, Nonstoichiometry, Diffusion and Electrical Conductivity in Binary Metal Oxides, Wiley-Interscience, New York, 1972, p. 203.
5 Per Kofstad, Nonstoichiometry, Diffusion and Electrical Conductivity in Binary Metal Oxides, Wiley-Interscience, New York, 1972, p. 1035.
6 W.K. Rudloff and E.S. Freeman, J. Phys. Chem., 74 (1970) 3317.
7 R. Furuichi, T. Ishii and K. Kobayashi, J. Therm. Anal., 6 (1974) 305.
8 M. Shimokwabe, R. Furuichi and T. Ishii, Thermochim. Acta, 21 (1977) 273.
9 M.R. Udupa, Thermochim. Acta, 13 (1975) 349.
10 M.R. Udupa, and G.K. Ramachandra, Thermochim. Acta, 9 (1974) 427.
11 M.R. Udupa, Thermochim. Acta, 15 (1976) 261.
12 M. Shimokawabe, R. Furuichi and T. Ishii, Thermochim. Acta, 20 (1977) 347.
13 M.N. Sastri and J.O. Hill, J. Therm. Anal., 11 (1977) 323.
14 S. Gal, K. Tomer, E. Pungor, G. Sooki-Toth and P. Horvath, J. Therm. Anal., 9 (1976) 241.

15 M.M. Barbooti and F. Jasim, Thermochim. Acta, 16 (1976) 402.
16 M.M. Barbooti and F. Jasim, Thermochim. Acta, 23 (1978) 103.
17 M.M. Barbooti, F. Jasim and S.K. Tobia, Thermochim. Acta, 21 (1977) 237.
18 M.M. Barbooti, F. Jasim and S.K. Tobia, Thermochim. Acta, 21 (1977) 399.
19 M.M. Barbooti and F. Jasim, J. Therm. Anal., 13 (1978) 563.
20 R.M. Al-Shukry and F. Jasim, Thermochim. Acta, 37 (1980) 97.
21 R.M. Al-Shukry and F. Jasim, Thermochim. Acta, 41 (1980) 281.
22 R.M. Al-Shukry and F. Jasim, J. Therm. Anal., in press.
23 K.R. Idan and F. Jasim, Thermochim. Acta, 39 (1980) 227.
24 K.R. Idan and F. Jasim, J. Therm. Anal., in press.
25 P.I. Fedorov and C.Y. Chang, Russ. J. Inorg, Chem., 11 (1966) 362.
26 P.D. Garn, Thermoanalytical Methods of Investigation, Academic Press, New York, 1965, p. 174.
27 T. Ishii, R. Furuichi and Y. Hara, J. Therm. Anal., 11 (1977) 71.
28 W.A. Roth and E. Becker, Z. Phys. Chem., Abt. A, 145 (1929) 461.
29 O. Glemser and U. Hauschild, Naturwissenschaften, 40 (1953) 317.
30 O. Glemser, U. Hauschild and F. Trupel, Z. Anorg. Alg. Chem., 277 (1954) 113.
31 B. Lorant, Z. Anal. Chem., 219 (1966) 256.
32 W.W. Wendlandt, Thermal Methods of Analysis, Wiley-Interscience, New York, 1974, 2nd edn., p. 175.
33 E.M. Barrall and L.B. Rogers, Anal. Chem., 34 (1962) 1106.
34 A. Rahmel, Arch. Eisenhuettenwes., 31 (1960) 59.